Mon. Not. R. Astron. Soc. **338,** 141–146 (2003)

The O4f + O6V eclipsing binary system Sk−67°105 in the Large Magellanic Cloud

Pablo G. Ostrov[1⋆] and Emilio Lapasset[2]

[1] *Facultad de Ciencias Astronómicas y Geofísicas, Universidad Nacional de La Plata, Paseo del Bosque S/N, 1900 La Plata, Argentina*
[2] *Observatorio Astronómico, Universidad Nacional de Córdoba, Laprida 854, 5000, Córdoba, Argentina*

Accepted 2002 August 30. Received 2002 August 16; in original form 2002 July 7

ABSTRACT

We present a new *V* light curve of the early type Magellanic eclipsing binary Sk−67°105, based on charge-coupled device images obtained at CASLEO. We perform an analysis of our data, together with published radial velocities, deriving the following masses and radii: $M_1 = 48.3$ $M_\odot$, $R_1 = 16.9$ $R_\odot$ for the O4f component and $M_2 = 31.4$ $M_\odot$, $R_2 = 13.8$ $R_\odot$ for the O6 component. We found that this system is the brightest member of a tight star cluster, belonging to an OB association.

Key words: binaries: eclipsing – stars: early type – stars: fundamental parameters – stars: individual: Sk−67°105.

1 INTRODUCTION

Sk−67°105 ($\alpha = 05^h\ 26^m\ 06^s$, $\delta = -67°\ 11'00''$, J2000) (Sanduleak 1969) is probably one of the most massive eclipsing binaries in the Large Magellanic Cloud (LMC). It is the brightest star embedded in the H II region N 50 (Henize 1956). Isserstedt (1975) performed *UBV* photoelectric photometry using the 61-cm telescope at La Silla, obtaining for Sk−67°105 $V = 12.42$, $B - V = -0.15$ and $U - B = -0.96$ mag. Later on, Mianes et al. (1977) published a *uvby* photoelectric study that also included Sk−67°105.

Niemelä & Morrell (1986) discovered that Sk−67°105 is a double-lined spectroscopic binary. Based on their spectrographic data, they classified the components of the system as O4f + O6V, determined a period of 3.301 d and derived minimum masses.

Haefner, Simon & Fiedler (1994) detected the optical light variability of Sk−67°105 and analysed their photoelectric photometry with the GRADUS code; they concluded that the system is near contact and obtained masses of ∼47 and ∼3 $M_\odot$. They also derived a period slightly longer than the spectroscopic one, but owing to the incompleteness of their data they could not decide which period was better. They also gave magnitudes and colours, namely $V = 12.42$, $B - V = -0.14$, $U - B = -1.03$, $V - R = -0.01$ and $V - I = 0.01$.

In this paper, we present a new *V* light curve for Sk−67°105, improve the value for the period and perform a new analysis with the Wilson–Devinney (WD) code (Wilson & Devinney 1971; Wilson 1990).

⋆E-mail: ostrov@fcaglp.edu.ar

2 OBSERVATIONS AND REDUCTIONS

We began our charge-coupled device (CCD) observations of Sk−67°105 in 1993 with the 2.15-m telescope at CASLEO,[1] using a Tektronix 1024 × 1024 CCD as detector. This gives a scale of about 0.27 arcsec pixel^{-1}, so we binned the CCD obtaining an equivalent scale of 0.54 arcsec pixel^{-1}. During this run, we observed through the Johnson's *B* and *V* filters.

In six subsequent runs during 1995, 1997, 1998, 1999, 2000 and 2001, we acquired CCD *V* images with the same telescope and detector but using a focal reducer. It gives a scale of 0.813 arcsec pixel^{-1} and a circular field of radius about 9 arcmin. During two photometric nights, in 1997 and 2001 we also acquired some *B* and *R* images for calibration purposes, together with frames of standard stars of the Selected Areas 92 and 98 from Landolt (1992).

Some 10 bias frames and flat-fields were acquired at the beginning and end of each observing night. The reduction of all the images was performed in the usual way (overscan and zero subtraction, flat-fielding) using the IRAF processing package.[2]

3 THE ENVIRONMENT AROUND SK−67°105

We combined the *B* and best-seeing *V* frames to obtain an averaged image for each band. We then performed a profile-fitting photometry on these combined images using stand-alone versions of DAOPHOT II and ALLSTAR (Stetson 1987; Stetson 1991). The derived

[1] Complejo Astronómico El Leoncito, operated under agreement between the Consejo Nacional de Investigaciones Científicas y Técnicas de la República Argentina and the National Universities of La Plata, Córdoba and San Juan.
[2] IRAF software is distributed by NOAO, operated by AURA for the NSF.

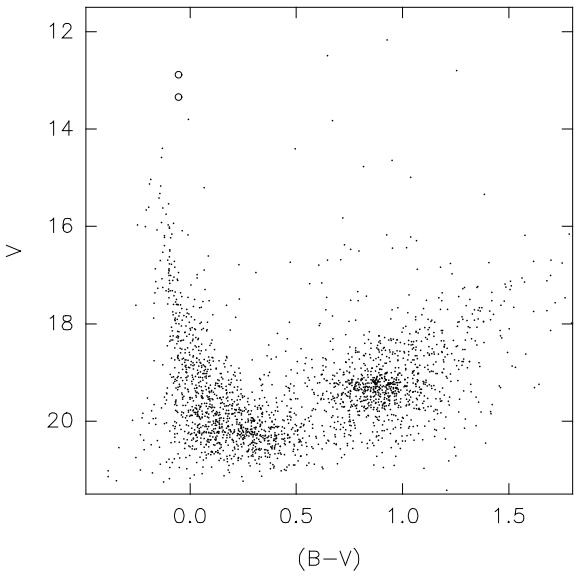

Figure 1. Colour–magnitude diagram for the field surrounding Sk−67°105. The two open circles represent the magnitude estimates for the components of Sk−67°105. Magnitudes and colours are not corrected for extinction.

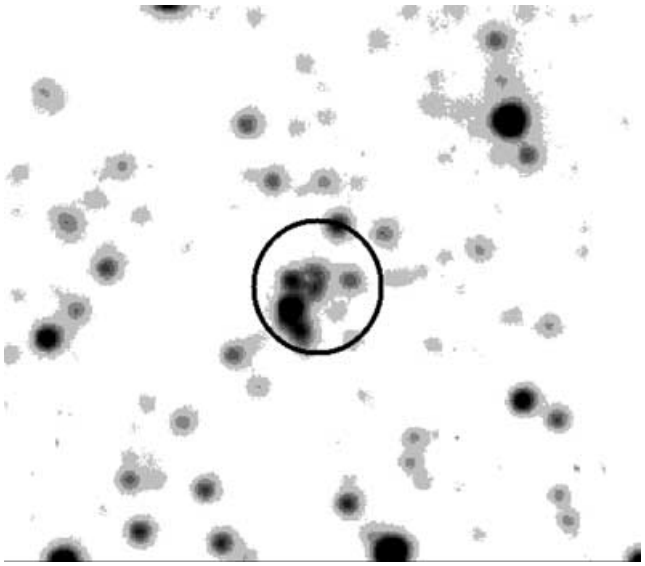

Figure 2. The close vicinity of the bright star Sk−67°105, which has been removed in order to show the adjacent faint compact cluster. The circle is about 15-arcsec radius.

colour–magnitude diagram revealed the presence of an OB association, the early O-type binary system being its most luminous member (Fig. 1).

The data obtained without the focal reducer during the first observing run, in 1993, did not reach the required quality to be included in the light curve, owing to severe instrumental problems. However, this data revealed that Sk−67°105 is the brightest star of a tight cluster. It was not possible to resolve that tight cluster in the images obtained with the focal reducer owing to undersampling, so we used the old images acquired during 1993 to attempt to resolve it. These images, by virtue of a more favourable scale allowed a better profile-fitting photometry, even with a poorer seeing. Still with a FWHM of about 3.3 arcsec, it was possible to resolve at least eight stars within an area of about 10-arcsec radius surrounding Sk−67°105. Our profile-fitting photometry revealed that the more prominent of these neighbours, located some 6.6 arcsec to the SE from Sk−67°105, is ∼3.2 mag fainter than it.

Fig. 2 shows in detail the immediate neighbourhood of Sk−67°105, which has been removed from the image in order to show the fainter stars of the tight stellar cluster.

4 LIGHT CURVE, PERIOD AND ABSOLUTE PHOTOMETRY

We derived the V light curve of Sk−67°105 from aperture photometry on the CCD images acquired between 1995 and 2000. We used an aperture of 4.75-arcsec radius, being the light contamination from the tight cluster of the order of 0.02 mag. We chose several field stars as local standards that were used to tie all the measurements to a unique instrumental system.

The light curve (displayed in Fig. 3) shows eclipses of equal depth but different shapes. The two maxima also differ by ∼0.027 mag. These features are probably a result of non-uniform brightness caused by gas streams and circumstellar material. Given the early types of the binary components, stellar winds and radiation pressure can produce strong interaction effects (Drechsel et al. 1995). From our observational data, we derived the following ephemeris:

$$P = 3.301\,61 \pm 0.000\,05$$

$$E_0 = 2451\,503.241 \pm 0.002,$$

which we used during the subsequent light and velocity curve analysis.

Table 1 presents the V-band aperture photometry, corrected by light contamination, together with the internal error (derived from the local standards), seeing and airmass. From the frames acquired during photometric nights, we derived absolute photometry for Sk−67°105, obtaining $V = 12.35 \pm 0.02$, $B - V = -0.053 \pm 0.02$ and $V - R = -0.032 \pm 0.02$, corrected to phase 0.25.

5 LIGHT AND VELOCITY CURVE ANALYSIS

Our V light curve, along with the radial velocities from Niemelä & Morrell (1986), were analysed using the Wilson–Devinney code (Wilson & Devinney 1971; Wilson 1990), which is suitable for modelling stars with Roche lobe geometry. The bolometric albedos A_1, A_2 and the gravity darkening exponents g_1, g_2 were assumed to be 1, as is expected for stars with radiative envelopes (Rucinski 1969; Lucy 1976). We adopted a square-root law for limb darkening (Díaz-Cordovés & Giménez 1992), using the coefficient values given by Díaz-Cordovés, Claret & Giménez (1995). We performed the light curve fit by adopting for the O4f star a temperature of 44 400 K (Chlebowski & Garmany 1991).

We found that the best fit to the light curve corresponded to an overcontact configuration, so we set the program operation to mode 1. In this mode, both potentials are kept identical ($\Omega_1 = \Omega_2$), the same as the gravity and limb-darkening coefficients and bolometric albedos. Besides, the temperature of the secondary T_2 is not a variable parameter, since it is assumed that the stars are in thermal contact.

Then, the set of adjusted parameters comprises the semimajor axis a, the inclination i, the potential of the common surface ($\Omega_1 = \Omega_2$), the mass ratio q and the primary luminosity L_1.

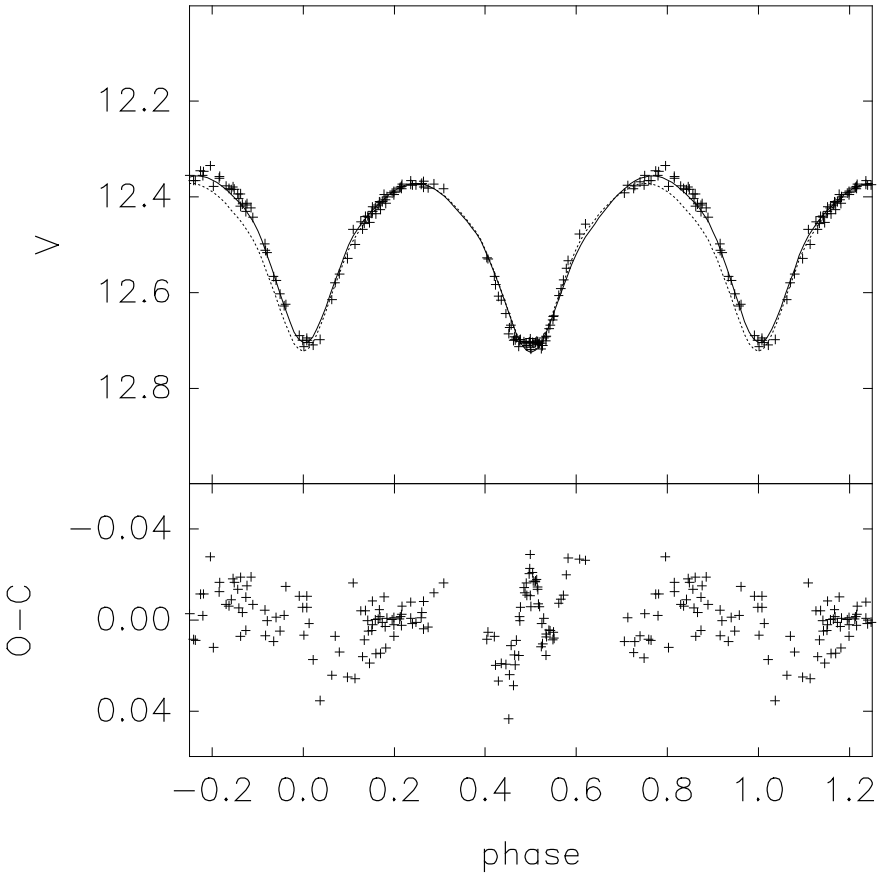

Figure 3. Top: the observed light curve of Sk−67°105, together with the spotted (full line) and unspotted (dotted line) modelled curves. Bottom: the (O–C) residuals of the spotted solution.

Since the observed light curve of Sk−67°105 is highly distorted, we accounted for the asymmetries placing bright and dark spots on the stellar surfaces.

Our fitted potential ($\Omega = 3.143\,79$), is very close to that corresponding to the double-contact configuration, ($\Omega = 3.1542$, with both stars filling exactly their corresponding Roche lobes); the differences between the two solutions are meaningless and – as is shown in Fig. 3 – the differences between the unspotted modelled light curve and the observed data are considerable; hence, we cannot rule out that this system is semidetached or even detached but, in both cases, close to contact. For this reason, we attempted to decouple the surface temperatures of both binary components setting the mode of operation to mode 3 of the WD programs, i.e. similar to mode 1 except that no thermal contact is assumed and T_2 can be fitted freely. The temperatures that we fitted for the secondary in mode 3 were some 800 K lower than those corresponding to thermal contact (quoted in Table 2). Taking into account the fact that the temperature affects mainly the ultraviolet (UV) brightness in such very hot stars, this derived temperature difference must be considered with caution. Anyway, it is compatible with the effective temperature expected for an O6V star (40 000–42 200 K, Martins, Schaerer & Hillier 2002; Chlebowski & Garmany 1991).

The obtained model parameters are displayed in Table 2, and the modelled radial velocity curve is shown in Fig. 4, together with the measurements from Niemelä & Morrell (1986).

6 DISCUSSION

Table 3 displays the derived masses, radii and bolometric magnitudes. For comparison, the corresponding radii for a double-contact configuration are $R_1 = 16.8\,R_\odot$ and $R_2 = 13.75\,R_\odot$ for the primary and secondary, respectively. It must be taken into account that the quoted errors reflect only the rms and fitting uncertainties. The radial velocities can also be affected by systematic errors (for example, Niemelä & Morrell derive $V_\gamma = 254 \pm 3$ and $285 \pm 10\,\mathrm{km\,s^{-1}}$, independently from the absorption lines of each binary component) therefore the real uncertainties of the stellar parameters could be larger.

The masses obtained from our solution are not significantly different from those derived by Haefner et al. (1994), but the radii are somewhat larger. These authors fitted an eccentric orbit in order to account for the light curve asymmetries, although they pointed out that such eccentricity is not real. Considering that our unspotted solution exhibits appreciable departures from the observed data points, we model the light curve by resorting to bright and dark spots and keeping the eccentricity zero. The differences between the two solutions are probably caused by the incompleteness of the light curve obtained by Haefner et al. (1994).

We presume that this system is now at the fast stage of case A mass transfer. The highly distorted shape of the light curve suggests strong interactions between stellar winds and streams of matter. There are no published evolutionary models suitable for such a massive close

Table 1. *V* light photometry of Sk−67°105.

HJD 2450000+	V	σ_i	FWHM (arcsec)	X	HJD 2450000+	V	σ_i	FWHM (arcsec)	X
767.646	12.361	0.009	3.26	1.38	1154.846	12.675	0.004	2.72	1.43
767.692	12.353	0.006	2.52	1.28	1155.603	12.365	0.007	2.69	1.34
767.766	12.347	0.007	3.32	1.23	1155.675	12.350	0.007	1.92	1.24
767.806	12.348	0.008	3.21	1.24	1155.713	12.342	0.005	1.88	1.23
767.847	12.345	0.006	3.01	1.29	1155.749	12.329	0.005	2.05	1.24
768.623	12.677	0.008	2.93	1.44	1155.777	12.339	0.005	1.93	1.28
768.680	12.674	0.007	2.40	1.30	1155.827	12.319	0.005	2.56	1.38
768.745	12.665	0.009	2.43	1.23	1155.852	12.320	0.006	2.78	1.46
768.801	12.623	0.006	2.41	1.24	1499.814	12.598	0.006	3.23	1.25
768.838	12.579	0.009	2.39	1.28	1500.582	12.365	0.005	3.41	1.59
769.638	12.351	0.005	2.78	1.39	1500.657	12.347	0.005	3.19	1.34
769.681	12.330	0.044	2.65	1.29	1500.730	12.349	0.006	3.51	1.24
769.788	12.357	0.020	3.57	1.23	1500.798	12.347	0.004	3.51	1.24
769.833	12.393	0.009	2.50	1.28	1500.843	12.355	0.004	3.27	1.29
770.609	12.502	0.006	2.35	1.48	1501.547	12.679	0.007	3.60	1.77
770.719	12.441	0.008	1.95	1.24	1501.563	12.684	0.007	2.90	1.68
770.768	12.427	0.008	2.50	1.23	1501.590	12.692	0.007	3.05	1.54
770.817	12.409	0.007	2.09	1.26	1501.608	12.680	0.007	3.55	1.47
770.848	12.400	0.009	2.08	1.30	1501.627	12.677	0.005	3.43	1.41
771.684	12.557	0.009	2.37	1.28	1501.645	12.681	0.005	2.97	1.36
771.703	12.581	0.006	2.49	1.26	1501.674	12.684	0.004	2.51	1.30
771.778	12.659	0.007	2.37	1.23	1501.724	12.648	0.004	3.11	1.24
771.813	12.673	0.007	2.69	1.26	1501.748	12.630	0.004	2.79	1.23
771.852	12.686	0.006	2.52	1.32	1501.809	12.565	0.004	2.96	1.25
772.641	12.349	0.008	2.93	1.36	1501.849	12.522	0.004	3.04	1.31
772.682	12.356	0.006	2.57	1.28	1502.566	12.308	0.008	3.53	1.65
772.758	12.349	0.005	2.90	1.23	1502.730	12.352	0.007	2.15	1.23
772.809	12.339	0.008	2.89	1.26	1502.785	12.367	0.007	2.20	1.23
772.858	12.329	0.012	3.58	1.34	1502.834	12.387	0.006	2.14	1.29
773.596	12.686	0.013	2.46	1.50	1502.862	12.396	0.014	2.23	1.34
773.658	12.683	0.009	2.08	1.32	1503.602	12.441	0.005	2.76	1.48
773.710	12.671	0.011	2.35	1.24	1503.692	12.414	0.008	2.76	1.26
773.795	12.588	0.011	3.26	1.24	1503.743	12.394	0.006	2.44	1.23
773.822	12.553	0.009	2.49	1.27	1503.796	12.385	0.006	2.77	1.24
773.850	12.534	0.023	3.26	1.33	1503.836	12.379	0.004	2.91	1.30
1149.802	12.576	0.010	1.98	1.29	1504.576	12.500	0.005	3.10	1.57
1149.832	12.601	0.007	2.38	1.35	1504.629	12.539	0.006	3.00	1.38
1150.682	12.356	0.013	2.11	1.24	1504.737	12.646	0.007	3.04	1.23
1150.844	12.353	0.009	1.93	1.39	1504.777	12.672	0.008	2.57	1.23
1151.618	12.669	0.004	1.99	1.33	1504.815	12.671	0.005	2.71	1.27
1151.671	12.676	0.004	1.91	1.25	1504.843	12.675	0.011	3.03	1.31
1151.735	12.664	0.003	1.89	1.23	1859.616	12.548	0.006	3.31	1.52
1151.788	12.622	0.002	2.08	1.28	1859.784	12.663	0.013	4.62	1.23
1151.858	12.547	0.006	2.17	1.44	1859.808	12.673	0.008	3.93	1.23
1152.665	12.334	0.006	2.29	1.25	1859.839	12.673	0.009	5.65	1.26
1152.711	12.350	0.004	2.21	1.23	1859.840	12.668	0.015	5.39	1.26
1152.752	12.358	0.005	2.01	1.24	1859.856	12.677	0.007	3.90	1.29
1152.803	12.377	0.005	1.94	1.31	1860.593	12.340	0.009	4.87	1.61
1152.832	12.388	0.004	1.98	1.37	1860.689	12.341	0.010	4.10	1.30
1152.856	12.404	0.006	2.17	1.44	1860.761	12.346	0.005	3.97	1.23
1153.647	12.472	0.020	1.81	1.27	1860.834	12.356	0.007	5.12	1.26
1153.693	12.425	0.005	1.68	1.23	1861.606	12.641	0.004	3.62	1.54
1153.737	12.413	0.004	1.94	1.23	1861.734	12.506	0.004	3.72	1.24
1153.769	12.408	0.004	2.16	1.26	1861.816	12.451	0.004	3.42	1.24
1153.825	12.383	0.006	2.39	1.36	1861.861	12.430	0.007	3.71	1.30
1153.858	12.368	0.004	2.90	1.46	1862.576	12.356	0.009	3.81	1.67
1154.614	12.503	0.009	2.23	1.32	1862.641	12.367	0.006	3.09	1.40
1154.707	12.589	0.005	2.34	1.23	1862.699	12.390	0.005	3.10	1.28
1154.742	12.617	0.005	2.27	1.24	1862.752	12.416	0.009	3.19	1.23
1154.805	12.665	0.006	2.45	1.32	1862.834	12.471	0.004	3.43	1.27
1863.558	12.429	0.004	2.82	1.76	1864.796	12.678	0.006	2.77	1.24
1863.587	12.416	0.003	2.41	1.60	1864.814	12.676	0.006	2.81	1.25
1863.616	12.404	0.007	2.64	1.47	1864.829	12.679	0.008	2.24	1.27

Table 1 – *continued*

HJD 2450000+	V	σ_i	FWHM (arcsec)	X	HJD 2450000+	V	σ_i	FWHM (arcsec)	X
1863.635	12.396	0.006	2.68	1.41	1864.845	12.679	0.005	2.46	1.29
1863.656	12.390	0.009	3.17	1.35	1864.860	12.668	0.011	2.70	1.32
1863.689	12.383	0.006	3.55	1.29	2212.810	12.485	0.002	2.40	1.23
1863.721	12.373	0.005	2.50	1.25	2212.819	12.490	0.002	2.72	1.23
1863.775	12.364	0.005	2.89	1.23	2212.866	12.540	0.002	2.89	1.25
1863.814	12.355	0.006	2.86	1.25	2213.683	12.387	0.002	2.41	1.39
1864.620	12.641	0.008	2.28	1.45	2213.744	12.369	0.002	2.05	1.27
1864.660	12.668	0.005	1.97	1.34	2213.798	12.351	0.002	2.61	1.23
1864.682	12.672	0.006	1.88	1.30	2214.731	12.687	0.002	2.94	1.28
1864.735	12.678	0.005	2.55	1.23	2214.807	12.691	0.002	2.12	1.23
1864.756	12.675	0.005	2.19	1.23	2214.843	12.674	0.002	2.21	1.24
1864.779	12.677	0.004	2.73	1.23					

Table 2. Model parameters.

a	$40.1 \pm 0.5\,R_\odot$
V_γ	$267 \pm 3\,km\,s^{-1}$
i	$68 \pm 1^\circ$
$q\ (M_2/M_1)$	0.65 ± 0.04
T_1	44400 K (adopted)
Ω_1	3.144 ± 0.080
T_2	44170 ± 1200 K
	Spots
In star 1	
Colatitude	90°
Longitude	21°
Ang. radius	28°
Temp. factor	1.2
In star 2	
Colatitude	90°
Longitude	343°
Ang. radius	28°
Temp. factor	0.92

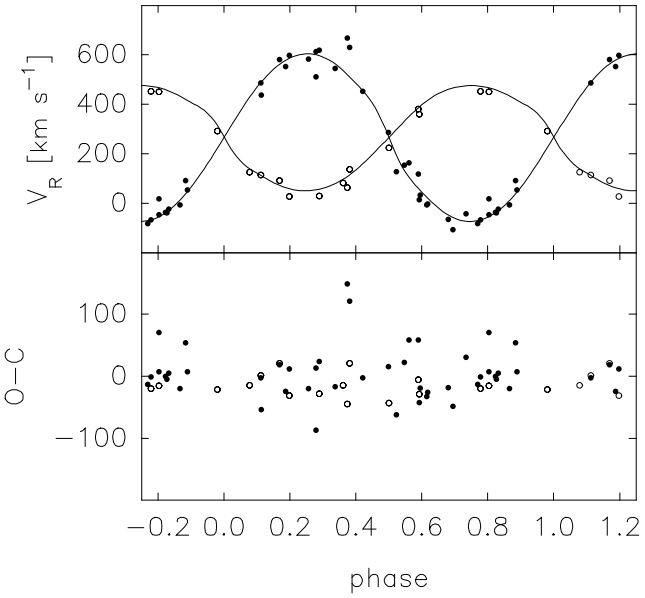

Figure 4. Top: the observed and modelled velocity curves for Sk−67°105. Bottom: the (O–C) residuals. Open circles correspond to the O4f star and filled ones to the O6 component.

Table 3. Star dimensions.

M_1	$48.3 \pm 0.7\,M_\odot$
R_1	$16.9 \pm 0.4\,R_\odot$
$M_{bol\,1}$	-10.21 ± 0.20
log g_1 [cgs]	3.67 ± 0.03
M_2	$31.4 \pm 0.7\,M_\odot$
R_2	$13.8 \pm 0.4\,R_\odot$
$M_{bol\,2}$	-9.75 ± 0.20
log g_2 [cgs]	3.65 ± 0.01

binary. A comparison with the evolutionary computations (for single stars) from Schaerer et al. (1993), suggests that the masses and radii of both components are in accord with tracks for more massive stars. However, such a comparison does not allow one to draw any conclusion concerning the evolution of isolated stars, because the radii that we derive depends on the Roche lobe geometry. On the other hand, considering its short period, it is presumably that this system has a very high mass-loss rate. Anyway, the evolution of such an early close binary is difficult to model, because of the importance of stellar winds and radiation pressure (Kondo, McCluskey & Guinan 2002).

We recently discovered an O3 III(f) + O5: binary system with a period of ∼2.2 d and masses of ∼100 $M_\odot$ and ∼50 $M_\odot$ (Ostrov 2002) and other O6V + O4III(f) of similar period with masses of only ∼26 and ∼16 $M_\odot$, respectively, (Morrell et al. 2002). Together with Sk−67°105, the very wide mass ranges of these close binaries are probably evidence of non-conservative mass transfer.

Given the strongly distorted light curve and the uncertainties in the temperature scale and bolometric corrections for very hot stars, this system is far from being adequate for accurate distance determinations. Anyway, since we have absolute photometry, we have derived a distance modulus, which must be considered only as indicative.

Assuming a $(B - V)_0 = -0.32$, the colour excess is $E_{B-V} = 0.267$. Adopting $R = 3.1$ (Koornneef 1982), the visual absorption is $A_V = 0.83$, and the distance modulus is 18.28 ± 0.21. This value is within the range of expected LMC distances. For example, although van den Bergh (2000) found a mean distance modulus of $(m - M) = 18.49$ from a series of recent determinations, that measurements comprise a range of ∼0.70 mag. Feast & Catchpole (1997) derive a distance modulus of 18.70 ± 0.10 using *Hipparcos* trigonometrical parallaxes of Cepheid variables to derive a zero-point for the period–luminosity relation, while Udalski et al. (1998b) obtain $(m - M) = 18.08 \pm 0.12$ by means of the red clump method.

Part of the discrepancies can be attributed to the systematic errors: another analysis of *Hipparcos* data yielded a distance modulus of 18.33 (Luri et al. 1998) and Cole (1998) decreased the red clump distance to $(m - M) = 18.36 \pm 0.17$, after considering age and metallicity effects. Regarding the use of eclipsing binaries as distance estimators, this method has the same problems inherent to any procedure that involves any class of standard candle: it is sensitive to errors in the estimation of absolute magnitudes of the stars (which depend on the temperature scale and bolometric corrections) and it is also affected by the reddening. Guinan et al. (1998), based on the light and velocity curve modelling of HV 2274, derive $(m - M) = 18.30 \pm 0.07$, and different estimations of the reddening yielded values from 18.22 to 18.46, for the same star (Udalski et al. 1998a; Nelson et al. 2000; Groenewegen & Salaris 2001). On the other hand, Ostrov, Lapasset & Morrell (2000) derive a distance modulus of ∼18.4 for HV 2543 and ∼18.7 for HV 2241 (Ostrov, Morrell & Lapasset 2001). In spite of all the uncertainties and sources of systematic errors, the range covered by the different distance estimations is compatible with what is expectable according to the physical size of the LMC.

ACKNOWLEDGMENTS

PGO is a visiting Astronomer at Complejo Astronómico El Leoncito, which is operated under agreement between the Consejo Nacional de Investigaciones Científicas y Técnicas de la República Argentina and the National Universities of La Plata, Córdoba and San Juan. The CCD and data acquisition system at CASLEO has been partly financed by R. M. Rich through US NSF Grant AST-90-15827. The focal reducer in use at CASLEO was kindly provided by Dr M. Shara. We would also like to thank to the referee for suggestions that helped us to improve the paper.

REFERENCES

Chlebowski T., Garmany C.D., 1991, ApJ, 368, 241
Cole A.A., 1998, ApJ, 500, L137
Díaz-Cordovés J., Giménez A., 1992, A&A, 259, 227
Díaz-Cordovés J., Claret A., Giménez A., 1995, A&AS, 110, 329
Drechsel H., Hass S., Lorenz R., Gayler S., 1995, A&A, 294, 723
Feast M.W., Catchpole R.M., 1997, MNRAS, 286, L1
Groenewegen M.A.T., Salaris M., 2001, A&A, 366, 752
Guinan E.F. et al., 1998, ApJ, 509, L21
Haefner R., Simon K.P., Fiedler A., 1994, A&A, 288, L9
Henize K.G., 1956, ApJS, 2, 315
Isserstedt J., 1975, A&AS, 19, 259
Kondo Y., McCluskey G.E., Jr, Guinan E.F., 2002, New Astron. Rev., 46, 1
Koornneef J., 1982, A&A, 107, 247
Landolt A.U., 1992, AJ, 104, 340
Lucy L.B., 1976, ApJ, 205, 208
Luri X., Gomez A.E., Torra J., Figueras F., Mennessier M.O., 1998, A&A, 335, L81
Martins F., Schaerer D., Hillier D., 2002, A&A, 382, 999
Mianes P., Prévot L., Prévot-Burnichon M.-L., Rousseau J., 1977, A&A, 58, 209
Morrell N.I., Ostrov P.G., Massey P., Gamen R., 2002, in preparation
Nelson C.A., Cook K.H., Popowski P., Alves D.R., 2000, AJ, 119, 1205
Niemelä V.S., Morrell N.I., 1986, ApJ, 310, 715
Ostrov P.G., 2002, MNRAS, 336, 309
Ostrov P.G., Lapasset E., Morrell N.I., 2000, A&A, 356, 935
Ostrov P.G., Morrell N.I., Lapasset E., 2001, A&A, 377, 972
Rucinski S.M., 1969, Acta Astron., 19, 245
Sanduleak N., 1969, Cerro Tololo Inter-American Obs. Contr. No. 89
Schaerer D., Meynet G., Maeder A., Schaller G., 1993, A&AS, 98, 523
Stetson P.B., 1987, PASP, 99, 191
Stetson P.B., 1991, in Grosbøl P.J., Warmel R.H., eds, 3rd ESO/ST-ECF Data Analysis Workshop. ESO, Garching, p. 187
Udalski A., Pietrzynski G., Wozniak P., Szymanski M., Kubiak M., Zebrun K., 1998a, ApJ, 509, L25
Udalski A., Szymanski M., Kubiak M., Pietrzynski G., Wozniak P., Zebrun K., 1998b, AcA, 48, 1
van den Bergh S., 2000, The Galaxies of the Local Group, Cambridge Astrophysics Series, Vol. 35. Cambridge Univ. Press, Cambridge
Wilson R.E., 1990, ApJ, 356, 613
Wilson R.E., Devinney E.J., 1971, ApJ, 166, 605

This paper has been typeset from a TEX/LATEX file prepared by the author.